Available online at www.sciencedirect.com

SciVerse ScienceDirect

Ceramics International 39 (2013) S487–S490

CERAMICS INTERNATIONAL

www.elsevier.com/locate/ceramint

# Electrical properties and phase of $BaTiO_3$–$SrTiO_3$ solid solution

S.W. Kim[a], H.I. Choi[a], M.H. Lee[b], J.S. Park[b], D.J. Kim[b], D. Do[b], M.H. Kim[b], T.K. Song[b], W.J. Kim[a,*]

[a]Department of Physics, Changwon National University, Changwon 641-773, Republic of Korea
[b]School of Nano and Advanced Materials Engineering, Changwon National University, Changwon 641-773, Republic of Korea

Available online 24 October 2012

**Abstract**

It has been known that $ABO_3$ type perovskite ferroelectrics, such as $BaTiO_3$ (BTO) and $SrTiO_3$ (STO), form a complete solid solution. In this study, $Ba_{1-x}Sr_xTiO_3$ (BST, $x=0.0$–$1.0$) solid solution were sintered by a solid-state reaction method using BTO and STO raw powders with appropriate chemical composition. The crystal structure was investigated by a Rietveld refinement method; Fullprof, using X-ray diffraction data. Within the reasonable goodness of fit, tetragonal symmetry was found in BST with $x \leq 0.2$, while BST with $x \geq 0.4$ were found to be cubic symmetry. However, $Ba_{0.7}Sr_{0.3}TiO_3$ was difficult to decide whether it is cubic or tetragonal because of large uncertainties after final fitting. The composition ratios calculated from the fitted occupancies match well with those measured by EDS within experimental uncertainties. Remnant polarizations of BST with $x < 0.3$ decrease with increasing Sr concentration. Furthermore, measured phase transition temperatures and maximum dielectric constant decrease as increasing Sr concentration. Measured electrical properties of BST were match well with the structural refinement investigations.


*Keywords:* B. X-ray methods; C. Dielectric properties; Solid state reaction; BST ceramics

## 1. Introduction

Barium strontium titanate, $Ba_{1-x}Sr_xTiO_3$ (BST), is one of ferroelectric materials with potential applications on microwave tunable devices, since it exhibits a high tunability in dielectric constant with applied electric field as well as a low dielectric loss at room temperature [1].

It has been known that $BaTiO_3$ (BTO) as a typical ferroelectric material has three phase transitions. While decreasing temperature, BTO has a cubic (paraelectrics) to tetragonal (ferroelectrics) phase transition around 398 K, which is known as a Curie temperature. BTO goes through further phase transitions from tetragonal to orthorhombic around 273 K and from orthorhombic to rhombohedral around 183 K [2]. Since BTO and $SrTiO_3$ (STO) were solid solution in the entire compositional range, BST were reported to have similar phase transitions with those of BTO [3].

It has been reported that the BST ceramics, including STO and BTO, usually exhibit sharp phase transition temperatures depending on the composition. Near the phase transition temperatures, maximum dielectric constant was observed and rapid decrease of the dielectric constant was common phenomena for all BST. The observed dielectric behaviours of the BST were not good for microwave applications, since temperature sensitive dielectric constant should affect greatly the impedance of the transmission line in real device environment. Therefore, less temperature sensitive dielectric materials with a high dielectric constant and a low loss in the microwave range may have more potential applications.

BST powders can be produced by three techniques; conventional solid-state reaction [4,5], sol–gel [6], and hydrothermal methods [7,8]. The sol–gel technique is beneficial to produce nano-sized powders. However, it is known to be an expensive and moisture-sensitive method [6,9]. Hydrothermal technique can produce size-controlled nano-crystalline powders at low temperature. However, it need to control the unexpected impurities caused by metal rests and/or reaction intermediates [7,8,10]. Unlike these

*Corresponding author. Tel.: +82 55 213 3428; fax: +82 55 267 0264.
*E-mail address:* kwj@changwon.ac.kr (W.J. Kim).

0272-8842/$ - see front matter © 2012 Elsevier Ltd and Techna Group S.r.l. All rights reserved.
http://dx.doi.org/10.1016/j.ceramint.2012.10.119

two techniques, the solid-state reaction technique needs calcinations at high temperature to form a crystalline. Obtained particle sizes after reaction are usually large with broad size distribution [11,12]. However, this method is relatively simple and easy to control the nominal composition.

In order to understand relation between structures and electrical properties, BST were sintered by solid-state reaction and investigated by an X-ray diffractometer. Fullprof has been used to refine the structure of BST using X-ray diffraction data with instrumental corrections. Dielectric and ferroelectric properties of BST were studied from measured hysteresis loops and dielectric constants.

## 2. Experimental procedure

$Ba_{1-x}Sr_xTiO_3$ ($x=0.0$–$1.0$) ceramics were fabricated from the mixture of BTO and STO. Raw powders were ball-milled in alcohol for 3 h with zirconia balls. After ball-milling, the powders were dried and calcined at 1000 °C for 3 h. The calcined powders were milled again for 3 h. After then the powders were dried and calcined again at 1100 °C for 3 h. 5 wt% of polyvinyl alcohol (PVA) was added to the calcined powders, and this mixture was desiccated at 90 °C for 30 min in a drying oven. And then samples were pressed into disks with 10 mm in diameter and 1 mm in thickness. The bulk ceramics were sintered at 1300 °C for 6 h. Before sintering, the samples were annealed at 500 °C for 30 min to remove PVA. Samples were polished to remove impurities on the surface and to make a desired thickness. For the electrical property measurements, electrodes were fabricated by silver paste on both surfaces of the samples and annealed at 650 °C for 30 min. Silicon (99.9%, Aldrich) powder was painted on the surface of samples before the XRD measurements for the angle reference.

The samples were structurally characterized using an X-ray diffractometer (RIGAKU, Miniflex II) with Cu$K_\alpha$ radiation ($lK_{a1}=1.540562$ Å, $lK_{a2}=1.544398$ Å). Data were collected from 20° to 80° of $2\theta$ with a step width of 0.02°. Phases in the samples were identified initially by comparing the known peak positions of STO and BTO reported in the JCPDS card number 35–0734 and 05–0626, respectively. Structure of BST was analyzed by a Rietveld refinement program; Fullprof, using X-ray diffraction data.

Dielectric constants were measured at 100 kHz in the temperature range from 25 K to 350 K using an impedance analyser (HP 4194A). Ferroelectric hysteresis loops were measured at 30 Hz using a Sawyer-Tower circuit with a function generator (FG300, Yokogawa), a digital oscilloscope (DL7100, Yokogawa) and a voltage amplifier (610E, Trek).

## 3. Results and discussion

Fig. 1 shows X-ray diffraction (XRD) patterns of the BST ceramics. Diffraction peaks were shifted to higher angles with increasing Sr contents due to the gradual decreases in lattice constants. A small amount of secondary phase was observed in samples with $x=0.4$–$0.7$, and identified as STO. Contribution of the secondary phase on the structural refinement of the main phase is negligible, since this can be subtracted by the Fullprof program.

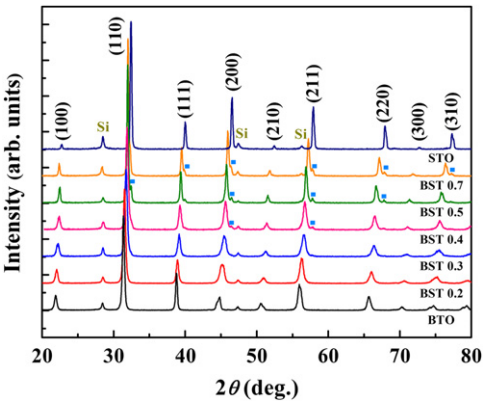


Fig. 1. The X-ray diffraction patterns of $Ba_{1-x}Sr_xTiO_3$ bulk ceramics with different composition. "■" indicates impurity phase. (For interpretation of the references to color in this figure legend, the reader is referred to the web version of this article.)

As a Rietveld refinement method, Fullprof is a powerful program for structure refinement in bulk. The diffracted X-ray intensity ($I_i^{calc}$) can be calculated by

$$I_i^{calc}=S_F\sum_{j=1}^{Nphases}\frac{f_j}{V_j^2}\sum_{k=1}^{Npeaks}L_k\left|F_{k,j}\right|^2S_j\left(2\theta_i-2\theta_{k,j}\right)P_{k,j}A_j+bkg_i \quad (1)$$

where $bkg_i$ is background, $S_F$ is beam intensity, $f_j$ and $V_j$ are phase volume and cell volume, $P_{kj}$ and $A_j$ are the preferred orientations and the absorption factor, $L_k$ is the Lorentz–polarization factor, $L_k$ is exhibited different value depend on the instrument, such as the geometry of monochromator, detector and sample position, *Npeaks* is a number of the peaks, and $S_j(2\theta_i-2\theta_{k,j})$ is line broadening [13].

The results of the structural refinements are summarized in Table 1. $\chi^2$ represent the statistical uncertainty for the final fitting to the measured total XRD data. $R_B$ (residue of Bragg factor) is uncertainty for the final fitting for each peak. If $\chi^2<4$, $R_B<8$, and Goodness of Fit (GofF) $<2$, the final structure used for refinement can be assumed as a reasonable one. Since BTO and STO were known as a tetragonal and a cubic structures with *P*4*mm* and *Pm*-3*m* space groups at room temperature, respectively [14,15], phases of the BST change from tetragonal to cubic [16] by increasing Sr concentration. However $Ba_{0.7}Sr_{0.3}TiO_3$ is difficult to decide whether it is tetragonal (*P*4*mm*) or cubic (*Pm*-3*m*) because of large $R_B$ values of 11.11% and 18.73%, respectively. This result might suggest that temperature of the tetragonal to cubic transition is close to the room temperature in $x=0.3$ composition.

By the result of the refinement, gradual changes of the lattice constants were observed. For tetragonal ($x<0.3$), lattice constants *a* and *c* decrease from 3.99567(1) Å to

Table 1
Fitting parameters of $Ba_{1-x}Sr_xTiO_3$ calculated using Fullprof.

| $x$ | Phase | $a$ | $c$ | $\chi^2$ | $R_B$ | GofF |
|---|---|---|---|---|---|---|
| 0.0 | Tetragonal | 3.99567(1) | 4.02590(3) | 2.34 | 6.22 | 1.48 |
| 0.2 | Tetragonal | 3.98886(5) | 4.01975(6) | 1.55 | 7.89 | 1.24 |
| 0.3 | Tetragonal | 3.97338(1) | 3.99599(2) | 2.86 | 11.11 | 1.69 |
| | Cubic | 3.97850(1) | | 5.67 | 18.73 | 2.28 |
| 0.4 | Cubic | 3.96621(1) | | 2.55 | 6.21 | 1.60 |
| 0.5 | Cubic | 3.95751(1) | | 3.05 | 6.62 | 1.69 |
| 0.7 | Cubic | 3.93897(1) | | 1.82 | 5.32 | 1.26 |
| 1.0 | Cubic | 3.90269(1) | | 1.74 | 3.15 | 1.24 |

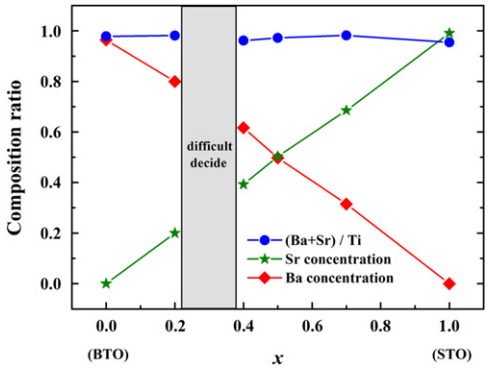


Fig. 2. Compositions of Ba and Sr, and the sum of (Ba+Sr)/Ti after final refinements. (For interpretation of the references to color in this figure legend, the reader is referred to the web version of this article.)

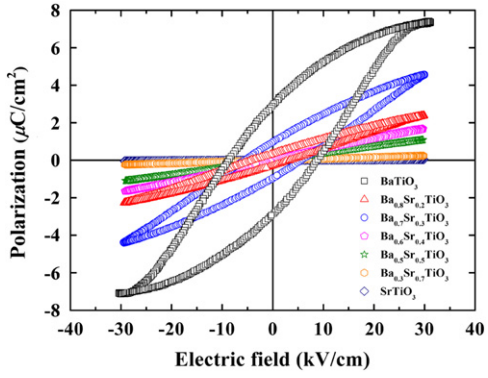


Fig. 3. *P–E* hysteresis loops of $Ba_{1-x}Sr_xTiO_3$ measured at room temperature. (For interpretation of the references to color in this figure legend, the reader is referred to the web version of this article.)

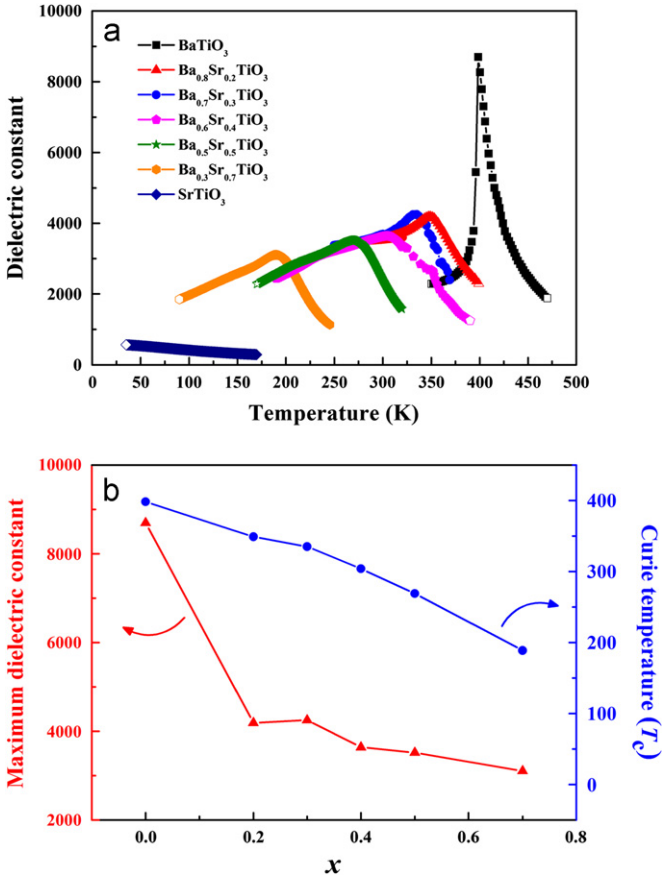


Fig. 4. (a) Dielectric constants properties and (b) maximum dielectric constant and curie temperature of $Ba_{1-x}Sr_xTiO_3$. (For interpretation of the references to color in this figure legend, the reader is referred to the web version of this article.)

3.97338(1) Å and from 4.02590(3) Å to 3.99599(2) Å, respectively. For cubic ($x > 0.3$), lattice constants $a$ decreases from 3.97850(1) Å to 3.90269(1) Å. The volume of the unit cell decrease gradually with increasing Sr content in accordance with the famous Vegard's law. These results are similar to previous reports [17].

The compositional ratios in ceramics were calculated by using the fitted occupancies [18] shown in Fig. 2. The calculated compositional ratio of (Ba+Sr)/Ti in the entire compositional range were close to 1. Furthermore, calculated Ba and Sr ratio are close to the nominal compositions.

Ferroelectric hysteresis loops of the BST measured by a Sawyer-Tower circuit operated with 30 Hz at room temperature were shown in Fig. 3. It was found that BST with $x < 0.3$ exhibit ferroelectric properties, while BST with $x > 0.3$ exhibit paraelectric properties. These are match well with the structural investigation; tetragonal for $x < 0.3$ and cubic for $x > 0.3$. For ferroelectric BST, remnant polarization $P_r$ and coercive electric field $E_c$ decrease with increasing Sr concentration. It has been reported that

dielectric constant peaks were observed at the tetragonal–cubic phase transition temperature ($T_c$). The temperature dependent dielectric constants of the BST are shown in Fig. 4(a). Measured $T_c$ and maximum dielectric constant at $T_c$ decrease with increasing Sr concentration as shown in Fig. 4(b), which are similar with previous reports [19]. However, STO ceramic were difficult decided $T_c$ and maximum dielectric constant because STO is a quantum paraelectric.

## 4. Summary

The BST ceramics were fabricated by a solid state reaction method. Lattice constants and cell volume decrease with increasing Sr concentration in the BST. By a Reitveld structural refinement using Fullprof, structures of BST in the entire compositional range were refined and found to be tetragonal ($x < 0.3$) and cubic ($x > 0.3$). However, the structure of $Ba_{0.7}Sr_{0.3}TiO_3$ is difficult to decide whether it is tetragonal or cubic because of the large uncertainties after final refinement. The measured $P_r$ of the ferroelectric BST with $x < 0.3$ decrease with increasing Sr concentration. On the other hand, BST with $x > 0.3$ exhibit paraelectric properties at room temperature. These observed electrical properties agree well with the structural analysis studied by structural refinement of the BST.

## Acknowledgements

This research was supported by basic Science Research Program through the National Research Foundation of Korea (NRF) funded by the Ministry of Education, Science and Technology (2011-0030805, 2011-0026395 and 2011-0027336).

## References

[1] W.J. Kim, W. Chang, S.B. Qadri, J.M. Pond, S.W. Kirchoefer, D.B. Chrisey, J.S. Horwitz, Microwave properties of etragonally distorted $(Ba_{0.5}Sr_{0.5})TiO_3$ thin films, Applied Physics Letters 76 (2000) 1185–1187.

[2] R.C. Pullar, Y. Zhang, L. Chen, S. Yang, J.R.G. Evans, P.Kr. Petrov, A.N. Salak, D.A. Kiselev, A.L. Kholkin, V.M. Ferreira, N.McN. Alford, manufacture and measurement of combinatorial libraries of dielectric ceramics Part II. Dielectric measurement of $Ba_{1-x}Sr_xTiO_3$ libraries, Journal of the European Ceramic Society 27 (2007) 4437–4443.

[3] L. Zhou, P.M. Vilarinho, J.L. Baptista, Dependence of the structural and dielectric properties of $Ba_{1-x}Sr_xTiO_3$ ceramic solid solutions on raw material processing, Journal of the European Ceramic Society. 19 (1999) 2015–2020.

[4] S. Tusseau-Nenez, J.-P. Ganne, M. Magilion, A. Morell, J.-C. Niepce, M. Pate, BST: effect of attrition milling on dielectric properties, Journal of the European Ceramic Society 24 (2004) 3003–3011.

[5] H.V. Alexandru, C. Berbecaru, A. Ioachim, M.I. Toacsen, M.G. Banciu, L. Nedelcu, D. Ghetu, Oxides ferroelectric $(Ba,Sr)TiO_3$ for microwave devices, Materials Science and Engineering: B 109 (2004) 152–159.

[6] A. Ries, A.Z. Simones, M. Cilense, M.A. Zaghete, J.A. Varela, Barium strontium titanate powder obtained by polymeric precursor method, Materials Characterization 50 (2003) 217–221.

[7] R.K. Roeder, E.B. Slamovich, Stoichiometry control and phase selection in hydrothermally derived $Ba_{1-x}Sr_xTiO_3$ powders, Journal of the American Ceramic Society 82 (1999) 1665–1675.

[8] S.B. Deshpande, Y.B. Khollam, S.V. Bhoraskar, S.K. Date, S.R. Sainkar, H.S. Potdar, Synthesis and characterization of microwave–hydrothermally derived $Ba_{1-x}Sr_xTiO_3$ powders, Materials Letters 59 (2005) 293–296.

[9] P. Pinceloup, C. Courtois, A. Leriche, B. Thierry, Hydrothermal synthesis of nanometer-sized barium titanate powders: control of barium/titanium ratio, sintering, and dielectric properties, Journal of the American Ceramic Society 82 (1999) 3049–3056.

[10] S.-F. Liu, I.R. Abothu, S. Komarneni, Baium titanate ceramics prepared from conventional and microwave hydrothermal powders, Materials Letters 38 (1999) 344–350.

[11] J.I. Clark, T. Takeuchi, N. Ohtori, D.C. Sinclair, Hydrothermal synthesis and characterization $BaTiO_3$ fine powders:precursors, polymorphim and properties, Journal of Materials Chemistry 9 (1999) 83–91.

[12] B.L. Newalkar, S. Komarneni, Microwave–hydrothermal synthesis and characterization of barium titanate powders, Materials Research Bulletin 36 (2001) 2347–2355.

[13] L.B. McCusker, R.B. Von Dreele, D.E. Cox, D. Louer, P. Scardl, Rietveld refinement guidelines, Journal of Applied Crystallography 32 (1999) 36–50.

[14] H.H. Weider, Electrical behavior of barium titanate single crystals at low temperatures, Physical Review 99 (1955) 1161–1165.

[15] W.J. Merz, The electric and optical behaviour of $BaTiO_3$ single-domain crystals*, Physical Review 76 (1949) 1221–1230.

[16] S.E. Moon, E.K. Kim, M.H. Kwak, H.C. Ryu, Y.T. Kim, W.J. Kim, Orientation dependent microwave dielectric properties of ferroelectric $Ba_{1-x}Sr_xTiO_3$ thin films, Applied Physics Letters 83 (2003) 2166–2168.

[17] N.J. Ridha, W.M.M. Yonus, S.A. Halim, Z.A. Talib, F.K.M. Al-Asfoor, W.C. Primus, Effect of Sr substitution and thermal diffusivity of $Ba_{1-x}Sr_xTiO_3$ ceramic, American Journal of Engineering and Applied 2 (2009) 661–664.

[18] A.M. Moustafa, E.A. El-Sayad, G.B. Sakr, Crystal structure refinement of $Cu_xAg_{1-x}InTe_2$ bulk material determined from X-ray powder diffraction data using the Rietveld method, Crystal Research and Technology 39 (2004) 266–273.

[19] J.H. Jeon, Effect of $SrTiO_3$ concentration and sintering temperature on microstructure and dielectric constant of $Ba_{1-x}Sr_xTiO_3$, Journal of the European Ceramic Society 24 (2004) 1045–1048.